Biochimica et Biophysica Acta 1843 (2014) 1076–1088

Contents lists available at ScienceDirect

Biochimica et Biophysica Acta

journal homepage: www.elsevier.com/locate/bbamcr

The c10orf10 gene product is a new link between oxidative stress and autophagy

Marcus W. Stepp, Rodney J. Folz, Jerry Yu, Igor N. Zelko *

Department of Medicine, University of Louisville, Louisville, KY 40202, USA
Department of Biochemistry and Molecular Biology, University of Louisville, Louisville, KY 40202, USA

ARTICLE INFO

Article history:
Received 5 July 2013
Received in revised form 21 January 2014
Accepted 6 February 2014
Available online 14 February 2014

Keywords:
Extracellular superoxide dismutase
DEPP
Autophagy
Aggresomes
Oxidative stress
Hypoxia

ABSTRACT

The human c10orf10 gene product, also known as decidual protein induced by progesterone (DEPP), is known to be differentially regulated in mouse tissues in response to hypoxia and oxidative stress, however its biological function remains unknown. We found that mice lacking extracellular superoxide dismutase (EC-SOD) show attenuated expression of DEPP in response to acute hypoxia. DEPP mRNA levels, as well as the activity of a reporter gene expressed under the control of the DEPP 5′-flanking region, were significantly upregulated in Hep3B and Vero cells overexpressing EC-SOD. Subcellular fractionation and immunofluorescent microscopy indicated that overexpressed DEPP is co-localized with both protein aggregates and aggresomes. Further biochemical characterization indicates that DEPP protein is unstable and undergoes rapid degradation. Inhibition of proteasome activities significantly increases DEPP protein levels in soluble and insoluble cytosolic fractions. Attenuation of autophagosomal activity by 3-methyladenine increases DEPP protein levels while activation of autophagy by rapamycin reduced DEPP protein levels. In addition, ectopic overexpression of DEPP leads to autophagy activation, while silencing of DEPP attenuates autophagy. Collectively, these results indicate that DEPP is a major hypoxia-inducible gene involved in the activation of autophagy and whose expression is regulated by oxidative stress.

1. Introduction

An adaptation of vertebrates to an oxygen-rich environment requires regulatory mechanisms responsive to a changing oxygen concentration. Oxygen sensing is also important in the development of many pathophysiological and diseased states. Molecular oxygen can be transformed into reactive and harmful byproducts in the course of normal metabolism and in response to hypoxia. These byproducts are represented by partially reduced forms of oxygen, and include superoxide anion radicals, hydroxyl radicals, and hydrogen peroxide. Collectively they are known as reactive oxygen species (ROS). There is now a large body of evidence suggesting that ROS not only can be deleterious to mammalian organisms, but also play important physiological functions such as regulating vascular tone, sensing of oxygen tension and modulating various signal transduction pathways [1].

Mammalian cells and tissues are protected against oxidative injury by multiple defense systems including antioxidant enzymes and small antioxidant compounds. The major class of antioxidant enzymes involved in maintaining homeostatic levels of superoxide species are the superoxide dismutase (SOD) family of metalloenzymes which catalyze the dismutation of superoxide radicals ($^{-}O_2^{\bullet}$) into hydrogen peroxide (H_2O_2) and molecular oxygen (O_2). Mammalian cells possess three distinct forms of SOD; copper–zinc SOD (CuZn-SOD or SOD1) located in the cytoplasm, manganese SOD (Mn-SOD or SOD2) found exclusively in the mitochondria, and extracellular SOD (EC-SOD or SOD3) present in the extracellular spaces [2,3]. EC-SOD is the principal enzymatic antioxidant in extracellular spaces and plays an important role in the protection of mammalian organisms against superoxide [4]. Expression levels of EC-SOD differ dramatically among tissues, but the highest expression is found in kidney, lung and heart [5,6]. In some human tissues such as uterus, umbilical cord, kidney, and arteries, EC-SOD enzyme activity equals or exceeds that from CuZn-SOD and Mn-SOD combined [7,8]. EC-SOD has been shown to provide protection against hyperoxic lung injury [9–12], bronchopulmonary dysplasia [11], influenza pneumonia [13], air pollution particle associated lung injury [14], hemorrhage induced-lung injury [15,16], radiation pneumonitis [17] and bleomycin lung fibrosis [18–20]. EC-SOD is involved in the regulation of angiogenesis due to suppression of hypoxia-inducible factor 1 (HIF-1α) and nuclear factor-κB (NFκB) expression [21] as well as repression of erythropoietin gene expression [22,23]. Thus, EC-SOD plays an important role in modulating oxidative stress under a variety of environmental exposure models that lead to the development of renal, pulmonary and cardiovascular diseases.

Abbreviations: DEPP, decidual protein induced by progesterone; GAPDH, glyceraldehyde-3-phosphate dehydrogenase; EC-SOD, extracellular superoxide dismutase; LacZ, β-galactosidase; ROS, reactive oxygen species

* Corresponding author at: 570 S. Preston Street, Baxter 1 Bldg., Room 221E, Louisville, KY 40202, USA. Tel.: +1 502 852 7632; fax: +1 502 852 2492.
E-mail address: igor.zelko@louisville.edu (I.N. Zelko).

http://dx.doi.org/10.1016/j.bbamcr.2014.02.003
0167-4889/

In the present study, we analyze the role extracellular reactive species play in the regulation of gene expression using mice deficient in EC-SOD. We found that the human c10orf10 gene product, also known as decidual protein induced by progesterone (DEPP) or fasting-induced gene (Fig) or fat-specific expressed gene (Fseg), was differentially regulated following the exposure of wild-type and EC-SOD knock-out mice to hypoxia. The full length cDNA for mouse DEPP consists of 2112 nucleotides and encodes a 205 amino acid long protein (GenBank accession number: AB022718). Computer assisted analysis using PROSITE PATTERN identified the putative t-synaptosome-associated protein receptor coiled-coil motif (SNARE) consisting of amino acids from 1 to 63. Further analysis using PSORT II program identified a second peroxisomal targeting signal RLLLSVAHL present at the N-terminus, however its importance remains to be verified. DEPP was first characterized as progesterone induced protein in endometrial stromal cells [24]. DEPP mRNA is expressed at a relatively high level in the lung, liver, heart, kidney, ovary, and arterial endothelial cells [24,25]. DEPP expression, at least at the mRNA level, is highly regulated by a variety of stimuli. DEPP steady-state mRNA levels are induced by hypoxia [26], progesterone [24], UV and ionizing radiation [27], by energy deprivation [28,29], highly selective RXR agonist LGD1069 [30], insulin [31], and by circadian rhythms [32]. DEPP is one of the 12 genes that can be used as a biomarker of phospholipidosis induced by a number of cationic amphiphilic drugs [33–35] and DEPP is a highly modulated biomarker found in human breast cells treated with bexarotene [30]. DEPP is the most highly induced gene in the uterus during human preterm and term labor [36]. It also has been shown that DEPP expression increases during tumor vascularization and wound healing [25]. Furthermore, Watanabe and coauthors reported that ectopic expression of DEPP results in activation of Elk-1 transcription factor and increased levels of phosphorylated mitogen-activated protein kinase (MAPK) Erk [24].

When the antioxidant protective systems are overwhelmed by oxidative stress it leads to the accumulation of oxidatively modified macromolecules and damaged cellular organelles. An effective pathway to eliminate these potentially toxic waste byproducts is through activation of autophagy, a process involving the cellular lysosomal degradation machinery [37]. Autophagy protects cells from oxidative damage by removing oxidatively damaged endoplasmic reticulum, mitochondria, and peroxisomes as well as aggregated proteins [38–40], and can facilitate cell survival during exposure to energy or oxygen deprivation [41]. However, excessive degradation of cellular components might also promote cell death through apoptosis or necrosis [42,43]. Thus, tight control of autophagy is required for cell survival in response to different kinds of stressors. Thus, it is not surprising that autophagy has been implicated in a variety of other biological processes, including aging, immunity, development, and cellular differentiation [44,45]. Increasing evidence suggests that ROS and oxidative stress can induce autophagy [46]. However, detailed molecular mechanisms that regulate autophagy by ROS are not well understood.

We have begun to explore the role that extracellular ROS play in regulating cellular signaling processes and gene expression. In the present study, we utilize both EC-SOD knock-out mice and transformed human cells overexpressing EC-SOD to demonstrate the important role EC-SOD plays in the regulation of DEPP expression and stability. In addition, we investigated the biological function DEPP plays in mammalian cells.

2. Materials and methods

2.1. Reagents

Oligonucleotides were obtained from Integrated DNA Technologies. UBEI-41 (4[4-(5-nitro-furan-2-ylmethylene)-3,5-dioxo-pyrazolidin-1-yl]-benzoic acid ethyl ester) was from Biogenova (Potomac, MA). All other chemicals and enzymes were from Sigma Chemical Co. (St. Louis, MO), or Invitrogen (Carlsbad, CA). Plasmids encoding pcECE-Foxo1-ADA, pECE-Foxo3a-ADA, and pECE-Foxo4-ADA were a gift from Dr. Burgering (Utrecht University, Netherlands).

2.2. Antibodies

The following antibodies that were used in this study: anti-LC3B, anti-Rab5, anti-Rab7, anti-Rab11, anti-phospho-S6K (Thr 389), S6K, Foxo1, Foxo3a, Foxo4 and anti-myc were from Cell Signaling Technology (Beverly, MA). Mouse monoclonal anti-GAPDH and goat polyclonal anti-Actin (C-11) antibodies were purchased from Santa Cruz Biotechnology (Santa Cruz, CA). In order to produce antibodies specific for DEPP, an antiserum was prepared against two distinct human DEPP peptides Ac-VRSISRLAQPTSVLDKAC-amide (FIP-1) and CEARMPGHSLARPPQDGQQS-amide (FIP-2) corresponding to amino acids 41–57 and 153–172 of the National Center for Biotechnology Information (NCBI) Reference Sequence (RefSeq) [record NP_008952]. These DEPP specific antibodies were affinity purified using resin conjugated peptides. Peptide synthesis, rabbit immunization and affinity purifications were performed by 21 Century Biochemicals (Marlboro, MA). Immunoblotting analysis indicated that the affinity purified IgG anti-FIP-1 peptide recognized human and mouse DEPP while IgG anti-FIP-2 peptide recognized only human DEPP.

2.3. Animals

All experiments involving animals were approved by the University of Louisville Institutional Animal Care and Use Committee. Homozygous EC-SOD KO mice (C57BL/6J) were generated by homologous recombination [9]. Control wild-type mice (C57BL/6J) were obtained from Taconic (Germantown, NY). All of the experiments in this study were performed using 6- to 8-wk-old male mice.

2.4. Cell culture and transfections

Vero (green monkey kidney epithelial cells), Hep3B (human hepatocellular carcinoma cell line), 769-P (human renal carcinoma), SV40 MES13 (mouse kidney mesangial cells) and HEK293 (human embryonic kidney cells) were obtained from ATCC (Manassas, VA). Vero, HEK293 and Hep3B cells were cultured in MEM medium supplemented with non-essential amino acids, sodium pyruvate and 10% fetal bovine serum (FBS).769-P cells were cultured in RPMI 1640 medium with 25 mM Hepes and L-glutamine containing 1.5 g/L sodium bicarbonate, 4.5 g/L glucose, 1 mM sodium pyruvate and 10% FBS. SV40 MES13 cells were cultured in DMEM/Ham's F12 medium with 14 mM Hepes and 5% FBS. Cells were maintained at 37 °C and 5% CO_2 in a humidified incubator.

Transfection assays were carried out using Lipofectamine2000 reagent (Invitrogen, Carlsbad, CA). Briefly, cells were seeded at 90% confluence on 24 well plates, incubated overnight before transfection, and then treated with Lipofectamine/DNA complexes for 5 h according to the manufacturer's instructions. Eighteen to twenty four hours after transfection, cell extracts were assayed for luciferase activity using a dual-luciferase reporter assay system (Promega, Madison USA). In experiments requiring protein detection, cells were lysed and analyzed using Western blot. All experiments were performed at least in triplicate, and the luciferase activity data were normalized to Renilla luciferase to control for differences in transfection efficiency by co-transfecting pRL-CMV plasmid (Promega, Madison USA).

2.5. Transfection of siRNAs

Expression of Foxo1 and DEPP was silenced using ON-TARGETplus pool of 4 different siRNAs (Thermo Scientific, USA). Non-targeting Pool ON-TARGETplus siRNA was used as negative control. HEK293 and Vero cells were transfected with siRNA using DharmaFECT 1 transfection reagent (Thermo Scientific, USA) according to the manufacturer's

protocol. The effect of siRNA on gene expression was analyzed after 24 h using qRT-PCR and Western blot.

2.6. Cell hypoxic exposures

For hypoxic exposures, the cells were seeded at 90% confluence on 35-mm dishes and incubated in complete medium containing 50 μM $CoCl_2$ or exposed to 1% oxygen with 5% CO_2. Total cellular RNA was isolated using Quick-RNA MicroPrep Kit (Zymo, Irvine, CA).

2.7. Exposure to hydrogen peroxide

Vero cells were exposed to an indicated concentration of hydrogen peroxide for 30 min and then exposed to either normoxia or hypoxia (1% O_2, 5% CO_2) for 4 h.

2.8. Mouse hypoxic exposures, RNA extraction and microarray analysis

EC-SOD KO and wild-type (C57BL/6J) mice were exposed to a continuous flow of normobaric hypoxia (7% oxygen) or room air (normoxia) for 4 h in an air-tight cabinet. Immediately after exposures, the mice were euthanized, and kidneys and brains were excised and used for the RNA isolation. Total RNA (20 μg) was extracted and purified using Trizol (Invitrogen, Carlsbad, CA). The quality of RNA was assessed using UV spectroscopy and an Agilent Lab-on-a-Chip 2100 Bioanalyzer (Agilent Technologies, Santa Clara, CA). RNA was labeled and co-hybridized with mouse MO36k oligonucleotide arrays printed by the Duke University Microarray Facility (Operon Mouse Oligo Set, version 4.0). Analysis was performed using GeneSpring v7.2 software (Agilent Technologies, Santa Clara, CA).

2.9. Quantitative RT-PCR

Total RNA was prepared from the cultured cells or mouse tissues using Trizol reagent (Invitrogen, Carlsbad, CA) or Quick-RNA MicroPrep Kit (Zymo, Irvine, CA). The synthesis of single stranded DNA from RNA was performed using SuperScript First-Strand Synthesis System for RT-PCR and random hexamers (Invitrogen, Carlsbad, CA), according to the protocol provided by the manufacturer. To quantitate the abundance of mRNA specific for EC-SOD and c10orf10, quantitative PCR was undertaken using the iCycler iQ™ Real-Time PCR Detection System (Bio-Rad, Hercules, CA) and an iQ SYBR® Green Master Mix. The PCR cycles were 95 °C for 3 min, then 40 cycles of 95 °C for 15 s, and 60 °C for 1 min. The EC-SOD primers were forward (5′-TGC CCC GCG TCT TCA G-3′) and reverse (5′-CCA AAC ATT CCC CCA AAG G-3′); the mouse DEPP primers were forward (5′-TAG ACT CCT GCC ACC CTG AC-3′) and reverse (5′-CTC TGG GCT GTG ACC TTG TC-3′); the human DEPP primers were forward (5′-GAC TGT CCC TGC TCA TCC AT-3′) and reverse (5′-CAC GTA GTC ATC CAG GCT AGG-3′); GAPDH primers were forward (5′-CAT GGA CTG TGG TCA TGA GT-3′) and reverse (5′-CCA TGT TCG TCA TGG GTG TGA-3′). PCR assays were run in triplicate, and analyzed gene mRNA levels were normalized to GAPDH mRNA levels.

2.10. Plasmids

The human DEPP gene's 5′-flanking sequences were generated by a standard PCR technique using Pfu Turbo polymerase (Stratagene, La Jolla, CA) and corresponding primer pairs containing Kpn I and Bgl II restriction sites for the 5′ and 3′ primers, respectively. The amplified DNA was cloned using pCR-Blunt II-TOPO kit (Invitrogen, Carlsbad, CA). The cloned EC-SOD promoter regions were recloned into pGL3-Basic vector (Promega, Madison, IN) at Mlu I and Bgl II restriction sites. The peroxisomal targeting signal 1 (PTS1) was created by annealing two phosphorylated oligonucleotides: sense 5′-GAT CTT CGT ACA AGT CCA AGC TGT AG-3′ and antisense 5′-AAT TCT ACA GCT TGG ACT TGT ACG AA-3′. The duplex was ligated into pDsRed1-C1 plasmid (Clontech, Mountain View, CA) at BglII and EcoRI restriction sites to create three amino acid sequence (Ser-Lys-Leu) at the C-terminal end of DsRed1 protein which resembled the putative PTS1 sequence. DNA sequencing confirmed the identity of all constructs.

2.11. Western blot

Whole cell lysates from Vero and HEK293 cells were prepared using RIPA buffer (50 mM Tris–HCl pH 8.0, 0.15 M NaCl, 0.1% SDS, 0.5% sodium deoxycholate, 1% NP-40) with protease and phosphatase inhibitors and separated on a 8–16% SDS-PAGE gel (Invitrogen, Carlsbad, CA), transferred to a PVDF membrane and stained using the corresponding antibodies. The specific protein bands were visualized using a chemiluminescence development kit (Cell Signaling Technology, Beverly, MA).

2.12. Immunofluorescence

Cells were seeded onto a Nunc Lab-Tek II Chamber Slide System (Sigma, St. Louis, MO) and fixed with 3.5% paraformaldehyde/PBS for 15 min in CO_2 incubator at 37 °C and then treated with blocking solution for 1 h at room temperature. The blocking solution contained 5% normal serum (from species in which secondary antibodies were produced) in PBS and 0.1% saponin. The same solution was used for diluting primary and secondary antibodies. The cells were incubated overnight with respective antibodies, washed with PBS and incubated for 1 h at room temperature with secondary antibodies (AlexaFluor 488 or AlexaFluor 594-conjugated antibody (Cell Signaling Technology, Beverly, MA)). After washing with PBS, the slides were incubated with DAPI, washed with PBS and then coverslipped with Prolong Antifade Reagent (Invitrogen, Carlsbad, CA) and analyzed with either confocal or wide-field fluorescent microscopy. Images were processed using Image J (National Institutes of Health, Bethesda, MA) and Adobe Photoshop (Adobe Systems, San Jose, CA).

2.13. Lysosome staining

Vero cells were transfected with GFP-DEPP and incubated for 18 h at 37 °C in CO_2 incubator. Lysosomes were stained using Lyso-ID Red Detection Kit from Enzo Life Sciences (Farmingdale, NY) for 20 min in CO_2 incubator.

2.14. Analysis of DEPP protein stability and degradation

To analyze DEPP stability Vero cells were transfected with plasmid encoding DEPP and 18 h later exposed to cycloheximide (50 μg/mL) and incubated for 30 min, 1, 2 and 3 h. Following exposure, the cells were washed once with ice-cold PBS and then lysed using Lysis buffer (10 mM Tris–HCl pH 7.5, 5 mM EDTA, 1% NP-40 (w/v), 0.5% deoxycholate, 150 mM NaCl with 0.25 mM PMSF) while being kept on ice for 10 min. Cells were scraped and lysates passed through a 25-gauge needle 10 times on ice to break up DNA. Inclusion bodies were collected by centrifuging lysates at 16,000 ×*g* for 30 min at 4 °C.

To analyze DEPP degradation by proteasomes, Vero or HEK293 cells were transfected with plasmid encoding DEPP and 18 h later were exposed to the proteosomal inhibitors MG132 (10 μM), lactacystin (10 μM) or ubiquitin ligase inhibitor UBEI-41 (50 μM). Total cellular lysates and soluble fractions or protein precipitates were prepared as described above.

2.15. Analysis of autophagy

HEK293 cells were transfected with plasmid encoding DEPP and exposed either to inhibitor of autophagy, 3-methyladenine (2.5 mM) or activator of autophagy, rapamycin (50 nM and 500 nM), for the indicated times. Total cellular extracts were analyzed for autophagosomal marker LC3-II using Western blot.

3. Results

3.1. The presence or absence of EC-SOD dramatically alters the magnitude of hypoxia-induced DEPP expression

To determine the effect of EC-SOD on the expression of hypoxia inducible genes, we exposed wild-type C57BL/6 and EC-SOD KO (same strain at least 10 generations) mice to room air or 7% oxygen for 4 h. Brain and kidney total RNA was isolated and differential expression of genes analyzed using microarray (Supplementary Fig. 1). DEPP was among several genes whose mRNA levels were altered by EC-SOD gene inactivation. To validate microarray data, we performed quantitative real-time PCR with primers specific for mouse DEPP. The beta-actin mRNA levels were also measured by real-time RT-PCR and used for normalization and to control for efficiency of tissue RNA isolation. At baseline (i.e., following exposure to room air (normoxia)), we did not find significant differences in DEPP mRNA levels between EC-SOD KO and wild-type mice (1.11 ± 0.18 vs. 1.15 ± 0.15 for kidney and 1.33 ± 0.31 vs. 0.92 ± 0.08 for brain (Fig. 1)). However, when the two groups of mice were exposed to 4 h of 7% hypoxia, dramatic differences were seen. Wild-type animals increased DEPP mRNA levels 24.5-fold to 27.2 ± 5.22 in the kidney and 9.6-fold to 12.78 ± 1.17 in the brain (Fig. 1). More importantly, EC-SOD KO mice significantly attenuated DEPP mRNA expression to only 5.23-fold (6.01 ± 1.78 R.U.) increase in kidney and 2.56-fold (2.35 ± 0.22 R.U.) in brain (Fig. 1). When compared to wild-type animals, EC-SOD KO mice showed a 78.7% reduction in DEPP induction in kidney and a 73.3% reduced induction in brain (from normoxia to hypoxia). Exposure of mice to hypoxia did not significantly change EC-SOD expression levels (Fig. 1C). These results demonstrate that the absence of EC-SOD attenuates DEPP induction by hypoxia or alternatively, the presence of EC-SOD augments DEPP induction by hypoxia in these cells.

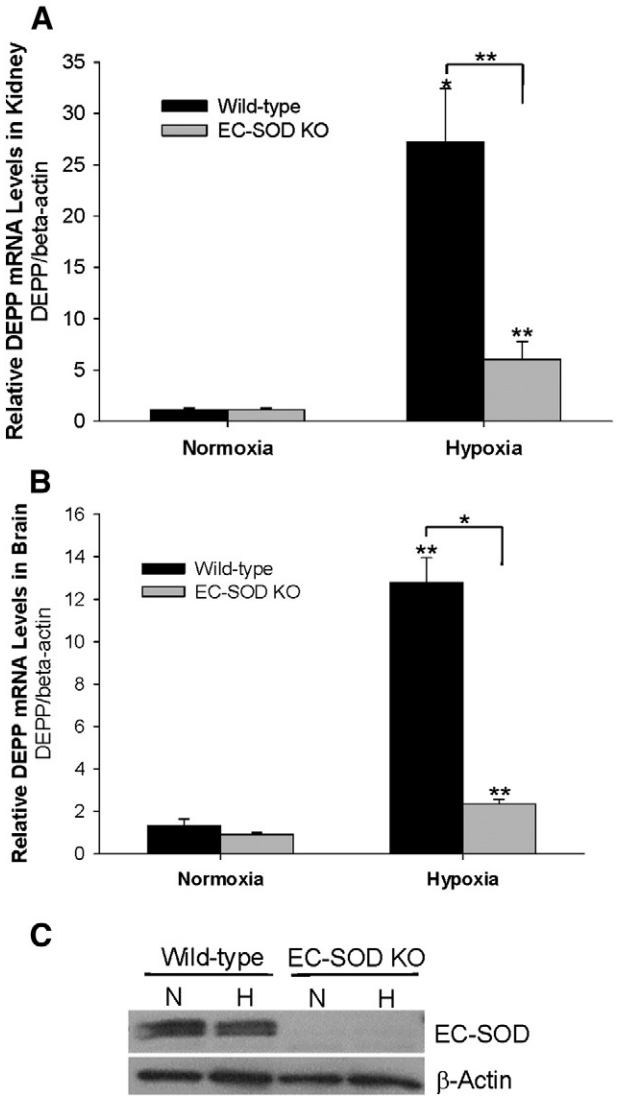

Fig. 1. EC-SOD regulates hypoxia-induced DEPP gene expression in mouse kidney (A) and brain (B). Mice were exposed to 7% oxygen (hypoxia) or room air (normoxia) for 4 h. Tissue total RNA was isolated and DEPP mRNA levels were determined by quantitative real-time PCR. Values were normalized to beta-actin (n = 4–5 mice for each group). Results shown are mean ± SD. Two asterisks represent $p < 0.05$, one asterisk represents $p < 0.001$; C, EC-SOD protein levels in the kidney of wild-type and EC-SOD KO mice exposed to hypoxia or normoxia.

3.2. DEPP induction by hypoxia

In order to study hypoxia inducible expression of DEPP, we exposed several cell lines to the hypoxic mimetic $CoCl_2$ (100 μM) or to hypoxia (1% O_2, 5% CO_2, 96% N_2) in an airtight humidified chamber for 4 h. Significant DEPP induction by hypoxia was observed only in Vero cells (Fig. 2A). The induction of DEPP by hypoxia in Vero cells is biphasic. Initially, DEPP mRNA levels increased after 1 h of hypoxia and reached a maximum of 10-fold at 4 h. The second peak of induction, up to 40-fold, was reached after 24 h of exposure (Fig. 2B). In order to determine the molecular mechanisms of DEPP hypoxia-dependent induction, we cloned 1 kb of its 5′-flanking region in front of the luciferase reporter gene in pGL3-Basic vector (Fig. 2C). This construct reporter activity showed a greater than 70-fold higher activity compared to the promoterless reporter following expression in Vero cells (Fig. 2D). Exposure to hypoxia did not activate this 1 kb DEPP promoter. This appears to not be due to the lack of HIF-1α, or some other hypoxia responsive transcription factor, because we did detect the induction of the erythropoietin gene in these cells (Fig. 2D).

3.3. Role of reactive oxygen species and EC-SOD in the regulation of DEPP expression in mammalian cells

To study the molecular mechanisms of EC-SOD dependent DEPP expression, we first developed and characterized a Hep3B cell line that permanently overexpresses EC-SOD. This cell line has been previously described [22]. We compared DEPP mRNA levels in Hep3B wild-type and EC-SOD overexpressing cells and found a 1.68-fold higher expression of DEPP in SOD3high vs. Hep3Bwt cells (Fig. 3A). However, the induction of endogenous DEPP mRNA by hypoxia (1% O_2, 5% CO_2, 94% N_2 for 4 h) in both cell lines was not detected. Nevertheless, overexpression of EC-SOD in Hep3B cells increases both DEPP mRNA levels as well DEPP promoter activity 1.68 and 1.42-fold, respectively (Fig. 3A and B). These data confirm that DEPP expression is regulated by EC-SOD and that *cis*-elements responsible for this regulation are located in the first 1000 bp of the DEPP 5′-flanking region.

The role of EC-SOD in hypoxia inducible expression of DEPP was further analyzed in Vero cells transfected with a plasmid encoding human EC-SOD. Overexpression of EC-SOD significantly increased DEPP expression in response to hypoxia (Fig. 3C and D). Since EC-SOD catalyzes the conversion of superoxide into hydrogen peroxide and oxygen, we decided to analyze the effect of hydrogen peroxide on basal and hypoxia inducible DEPP expression. Vero cells were exposed to different concentrations of hydrogen peroxide and then exposed to either normoxia or hypoxia for 4 h. Hydrogen peroxide, at a concentration 0.75 mM, induced DEPP expression up to 3-fold (Fig. 3E). However, no significant effects of hydrogen peroxide, on fold of DEPP induction by hypoxia, were observed. These data indicate that EC-SOD might mediate its effects on DEPP expression via an elevation in the production of hydrogen peroxide.

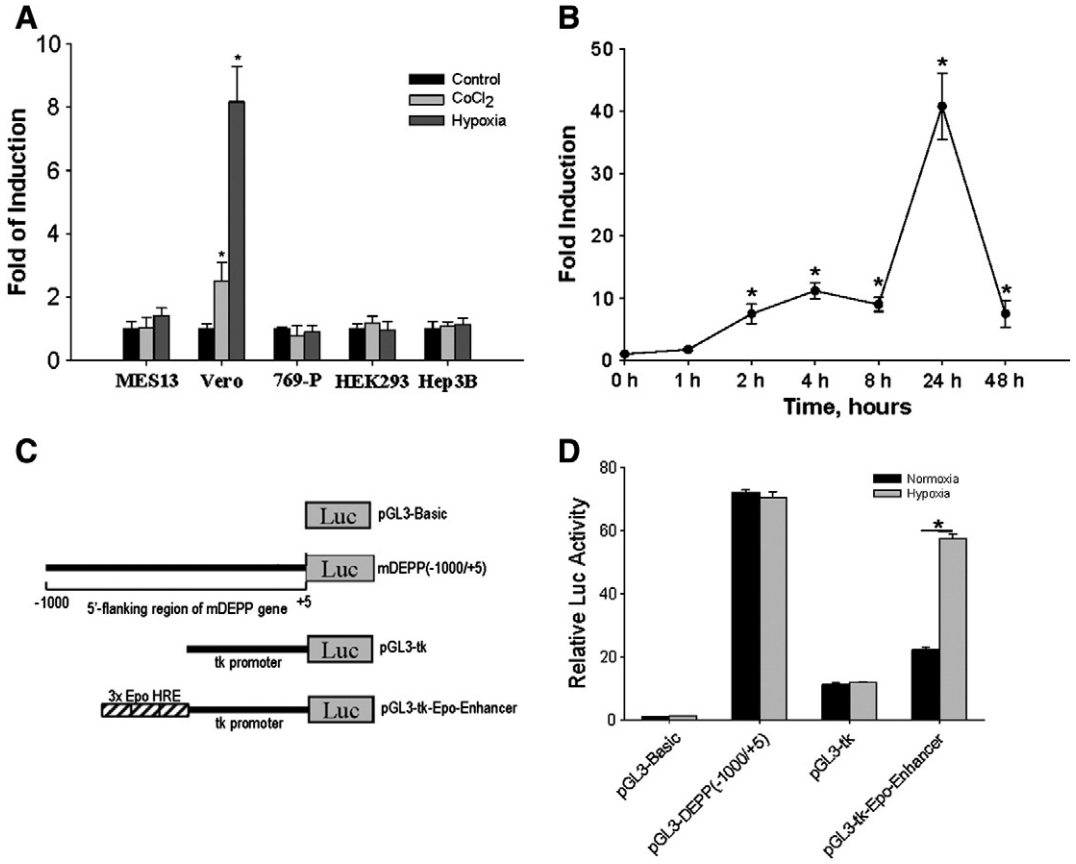

Fig. 2. Regulation of DEPP expression by hypoxia in human cells. A, Different mammalian cells were exposed to either hypoxia (1% oxygen for 4 h) or $CoCl_2$ (100 μM for 4 h). Following exposure total RNA was extracted and DEPP expression was analyzed using quantitative RT-PCR. B, Time-course of DEPP mRNA induction by hypoxia in Vero cells. Vero cells were exposed to hypoxia (1% O_2, 5% CO_2, 94% N_2) for time indicated. After hypoxic exposure total RNA was isolated and relative abundance of DEPP mRNA was analyzed using quantitative RT-PCR. Values were normalized to GAPDH. *$p < 0.01$; C, Schematic representation of mDEPP 5′-flanking region promoter/reporter constructs and hypoxia-responsive construct utilizing the three repeats of erythropoietin (Epo) hypoxia responsive elements (HRE) cloned in front of thymidine kinase (tk) promoter. D, Effect of hypoxia (1% O2, for 4 h) on the reporter activities of constructs depicted in panel C when transfected into Vero cells. *$p < 0.05$ between normoxia and hypoxia. Relative DEPP mRNA levels were detected using quantitative RT-PCR. Results shown are mean ± SD from at least two independent experiments, each performed in triplicate.

3.4. Regulation of DEPP expression by Foxo transcription factors

In order to gain insights into the transcriptional regulation of DEPP, we analyzed the role of the Foxo subfamily of forkhead transcription factors in the activation of DEPP gene expression. Using microarray analysis, it has been shown that ectopic expression of Foxo3a (FKHRL1) in prostate tumor cells increased DEPP mRNA levels by 506-fold [47]. To confirm the role of Foxo in the regulation of DEPP expression, we transfected HEK293 and Vero cells with plasmids encoding constitutively active mutant forms of Foxo1 (FKHR), Foxo3a (FKHRL1) and Foxo4 (AFX). Overexpression of Foxo1 and Foxo3a increased DEPP mRNA 9.8-fold and 2.2-fold, respectively in HEK293 cells (Fig. 4A and C). Ectopic expression of Foxo1 and Foxo3a in Vero cells induced DEPP expression 1.5-fold and 2.6-fold, respectively (Fig. 4B and C). However, overexpression of Foxo1 and Foxo3a transcription factors did not affect hypoxia induction of DEPP when compared to controls. For example, while transfection of Vero cells with Foxo3a significantly increased steady-state levels of DEPP mRNA in normoxia conditions, there was no additional augmentation of induction under hypoxia conditions (Fig. 4B). Foxo4 overexpression showed no effect on DEPP mRNA levels in either cell lines.

In order to identify the location of *cis*-elements involved in Foxo1 dependent induction of DEPP, we transfected HEK293 and Vero cells with plasmids expressing a reporter construct under control of the DEPP promoter. Foxo1 overexpression in both cell lines activated DEPP promoter by 3-fold, while a control promoterless construct was not activated (Fig. 4D). Next, we analyzed the effects of Foxo1 silencing on DEPP basal and hypoxia inducible expression. Foxo1 specific siRNA attenuated Foxo1 levels by at least 50% in both cell lines as detected using qRT-PCR (data not shown) and Western blot (Fig. 4E). Moreover, silencing of Foxo1 reduced DEPP mRNA levels by 51% under normoxic conditions and by 48% under hypoxic conditions in Vero cells (Fig. 4F). Interesting, no significant effects of Foxo1 siRNA on DEPP mRNA levels were observed in HEK293 cells. These results indicate that Foxo1 and Foxo3a transcription factors are potent regulators of DEPP expression in mammalian cells.

3.5. DEPP intracellular localization

In order to gain insights into a possible biological role for DEPP, we first searched for homology between amino acid sequences of DEPP and any known proteins or protein structural motifs. As shown in Fig. 5A, the DEPP amino acid sequence is highly conserved between a variety of species including human, chimp, dog, cow and rodent. However, no significant homology was found with any known protein or structural motif. Only two weak homologies were found for putative t-synaptosome-associated protein receptor coiled-coil motif (SNARE) and to peroxisomal targeting signal (PTS2) (Fig. 5A). The SNARE motif is a domain of approximately 60 amino acids involved in vesicle fusion and transport. PTS2 is a signal peptide responsible for peroxisomal localization of proteins. Transient transfection of mammalian cells with the plasmid encoding DEPP protein fused to the green fluorescent protein (GFP) revealed punctate strong signals scattered throughout the

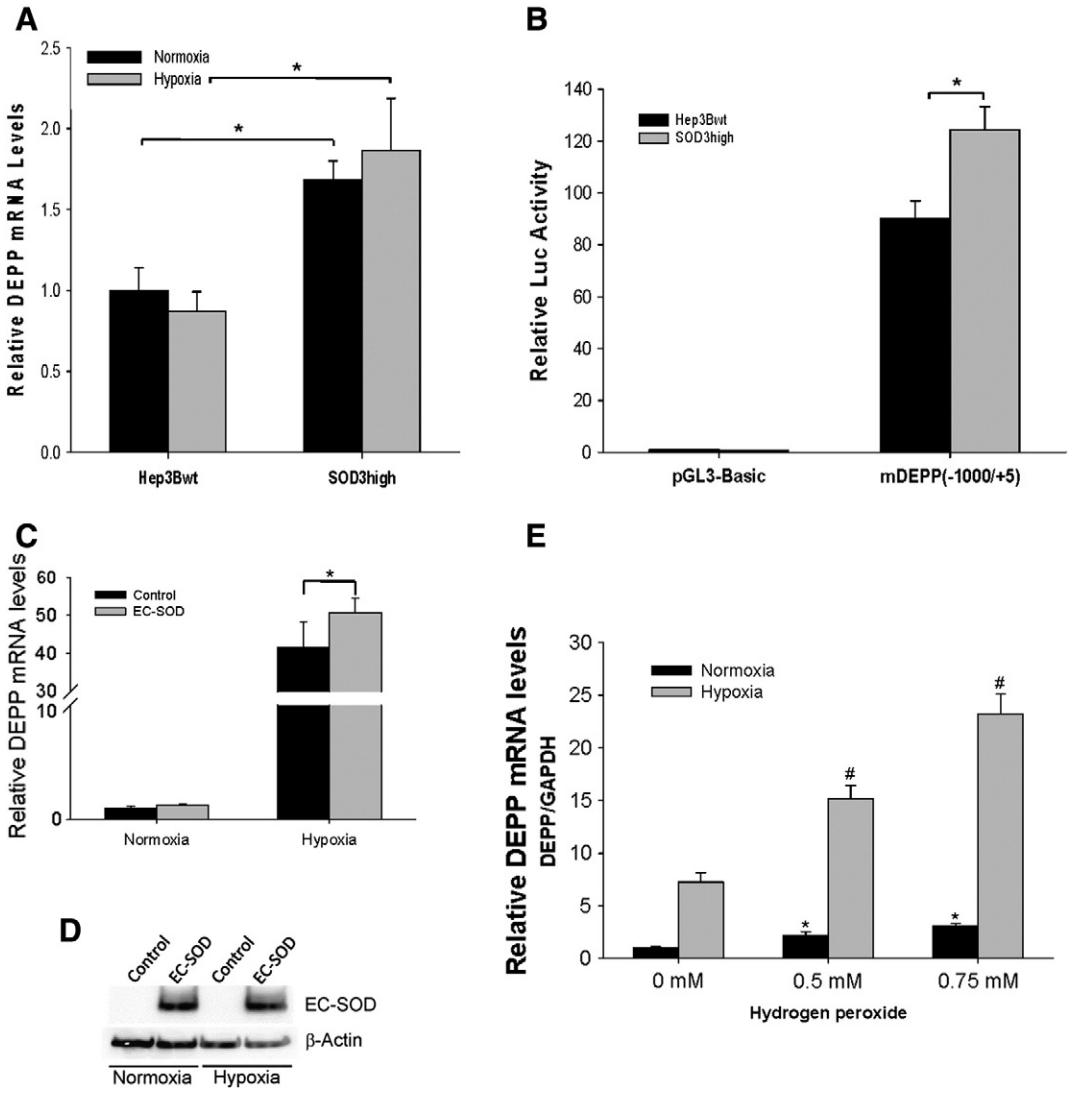

Fig. 3. Regulation of DEPP expression by reactive oxygen species. A, Hep3Bwt and overexpressing EC-SOD (SOD3high) were exposed to normoxia (21% O_2, 5% CO_2, 74% N_2) and hypoxia (1% O_2, 5% CO_2, 94% N_2) for 4 h. DEPP mRNA levels were analyzed using quantitative RT-PCR and normalized to GAPDH expression, $^*p < 0.01$ B. Activity of mDEPP promoter/reporter construct in Hep3Bwt and SOD3high cells, $^*p < 0.001$. C, Vero cells were transiently transfected with plasmid encoding EC-SOD and then exposed to hypoxia for 24 h. DEPP mRNA levels were determined using qRT-PCR ($N = 6$), $^*p < 0.05$. D, Western blot of EC-SOD overexpression in Vero cells. E, Vero cells were exposed to different concentrations of hydrogen peroxide for 30 min and then exposed to normoxia or hypoxia (1% O_2, 5% CO_2) for 4 h. DEPP mRNA levels were quantified using qRT-PCR and then normalized to GAPDH expression. Results shown are mean ± SD from three independent experiments. $^*p < 0.01$ compared to 0 mM H_2O_2 normoxia, $^\#p < 0.01$ compared to 0 mM H_2O_2 hypoxia.

cytoplasm with the large bodies of fluorescence juxtaposed to the nucleus (see Supplementary video). The low intensity green fluorescence signal was evenly distributed between nucleus and cytoplasm. Taking into consideration that DEPP shares some homology with the SNARE domain involved in vesicular trafficking, we evaluated for colocalization of DEPP specific punctate staining with endosomes. Because the main transport vesicles in the cell are endosomes, we analyzed colocalization of DEPP with endosomes using antibodies specific for the Rab family of proteins. The Rab family of proteins is part of the Ras superfamily of small GTPases that function as regulators of vesicle formation, vesicle movement and membrane fusion [48]. We found that DEPP was not colocalized with Rab proteins (Rab5 (sorting endosomes), Rab7 (late endosomes), or Rab11 (recycling endosomes)). On the other hand, complete colocalization of signals were observed when DEPP protein was detected using fused green fluorescent protein (GFP) and antibodies specific for DEPP (Fig. 5B). In addition, we analyzed the importance of the putative peroxisome targeting peptide located in the N-terminal part of DEPP for translocation of newly synthesized protein into peroxisomes. We found no significant colocalization of DEPP with peroxisomes (Fig. 5B).

3.6. Association of DEPP with aggresomes

The distinct punctate staining of cells overexpressing GFP-DEPP protein and additional juxtanuclear localization of large fluorescent complexes suggested that these localized signals can represent protein aggregates. Indeed, GFP-DEPP fluorescent signal was colocalized with aggresomes (Fig. 6A). However, no overlapping fluorescent signals between DEPP aggregates and lysosomes were detected (Fig. 6B). The lack of colocalization between GFP-DEPP and lysosomal marker may be due to the acid-labile properties of EGFP protein which has a pKa of 6.0. EGFP protein becomes non-fluorescent when transferred into an acidic environment of lysosomes where the pH is about 4.7 [49]. Nevertheless, these data indicate that DEPP, overexpressed in mammalian cells, forms large aggregates that are sequestered in the juxtanuclear aggresomes. Aggregation of DEPP can explain the significantly lower levels of DEPP protein compared to beta-galactosidase (Fig. 6C). It is likely that DEPP aggregates form inclusion bodies which undergo rapid degradation through proteosomal and/or autophagosomal pathways. As expected, overexpression of DEPP in mammalian cells leads to its distribution between soluble and insoluble (protein aggregate enriched) fractions

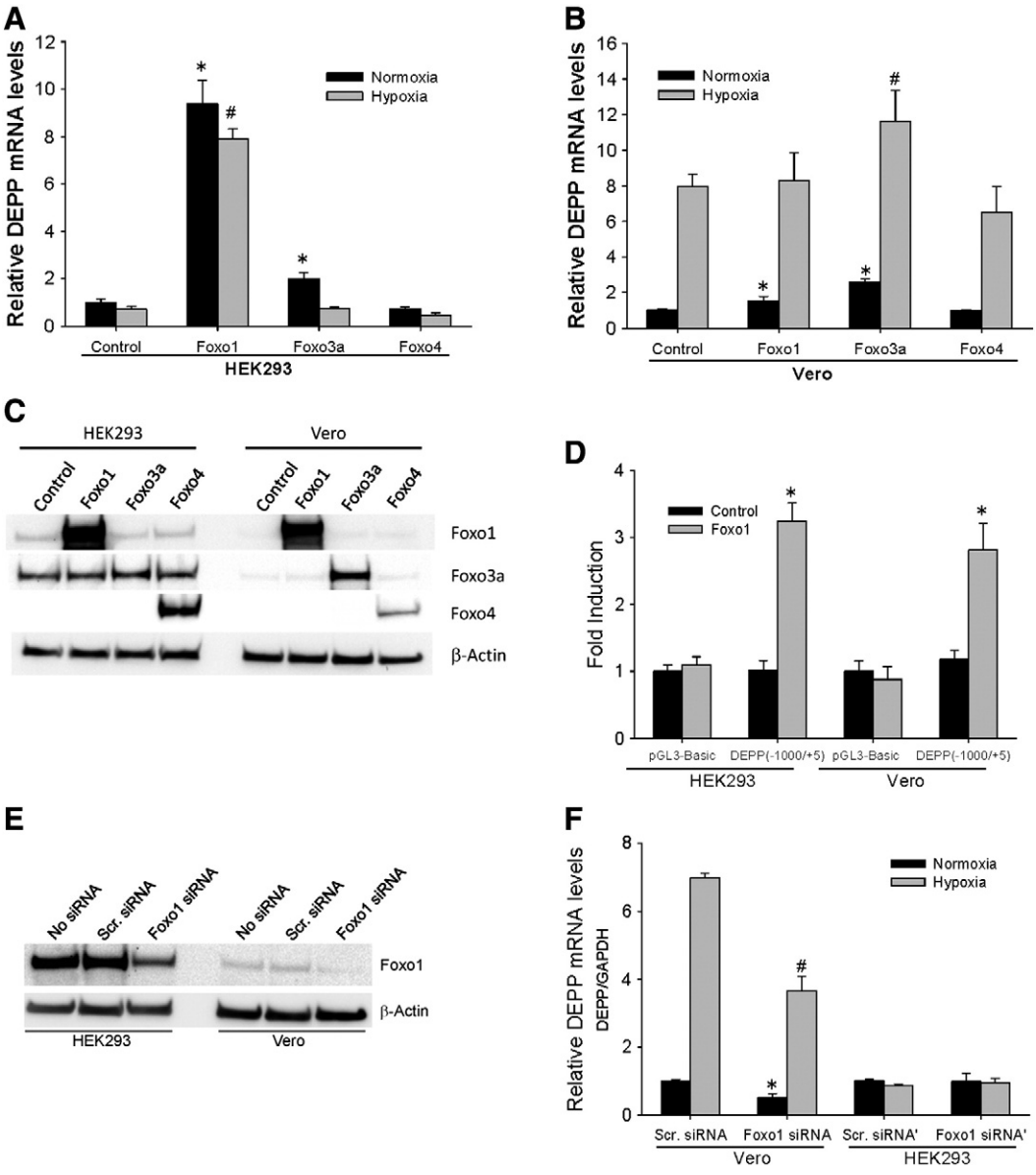

Fig. 4. Regulation of DEPP expression by Foxo transcription factors. A–B, Ectopic expression of Foxo1 and Foxo3a induced DEPP expression. HEK293 (A) and Vero (B) cells were transiently transfected with plasmids encoding constitutively active Foxo1, Foxo3a and Foxo4 transcription factors. Twenty hours later cells were exposed to either normoxia or hypoxia (1% O2) for 4 h. The total RNA was isolated and relative abundance of DEPP mRNA was analyzed using quantitative RT-PCR. *$p < 0.01$ compared to control (normoxia); #$p < 0.05$ compared to control (hypoxia). C, Western blot of Foxo proteins transiently transfected into HEK293 and Vero cells. D, Vero and HEK293 cells were transfected with pGL3-Basic or pGL3-DEPP-Promoter plasmids and then co-transfected with plasmid encoding Foxo1 transcription factor. Luciferase activity was analyzed 24 h after transfection and normalized to Renilla activity. Data are expressed as fold of induction. *$p < 0.001$ compared to control. E, HEK293 and Vero cells were transfected with siRNA pool specific to Foxo1. For a control we used non-transfected cells and cells transfected with non-targeting pool of siRNAs (scrambled siRNA). Effect of siRNA transfections on Foxo1 expression was analyzed using Western blot with Foxo1 specific antibodies. F, Effect of Foxo1 silencing on DEPP basal and hypoxia inducible expression in HEK293 and Vero cells was analyzed using qRT-PCR. DEPP expression was normalized to GAPDH. *$p < 0.01$ compared to scrambled siRNA (normoxia); #$p < 0.05$ compared to scrambled siRNA (hypoxia). Results shown are mean ± SD from at least two independent experiments, each performed in triplicate.

(Fig. 6D). Moreover, treatment of cells using the protein synthesis inhibitor cycloheximide significantly attenuates the intensity of bands in soluble fractions, while levels of insoluble protein were reduced only marginally. The cytosolic GAPDH protein was localized exclusively in soluble fractions and treatment with CHX did not significantly change it levels.

Fig. 5. Alignment and intracellular localization of DEPP. A, The multiple alignments of amino acid sequences of DEPP from different species. The amino acid sequences of DEPP from cow, dog, human, chimpanzee, mouse and rat were aligned. Identical residues in DEPP orthologous are shaded with yellow, conservative residues are shaded with blue and block of similar residues are shaded with green. Two weak homologies were found in N-terminal part of DEPP for peroxisomal targeting signal and for putative t-synaptosome-associated receptor coiled-coil motif (SNARE-motif). The following NCBI RefSeq records were used for DEPP orthologues: human (NP_008952.1), cow (NP_001039980.1), dog (XP_534951.1), mouse (NP_666092), rat (NP_001019505.2), and chimpanzee (XP_001158796.1). B, DEPP does not colocalize with endosomes. Vero cells were transfected with the plasmid encoding DEPP fused with green fluorescent protein (GFP). After fixation with paraformaldehyde cells were immunostained with antibodies specific for Rab family of proteins. Rab proteins are GTPases located on endosomal membrane and involved in many aspects of vesicle-mediated transport. Rab5 is a marker of early endosome, Rab7 is a marker of early and late endosomes and Rab11 is a marker of late endosomes. The colocalization of signal obtained from DEPP-GFP and immunofluorescent staining using antibodies specific for DEPP is shown in the lower panel. DEPP does not colocalize with peroxisomes. DEPP-GFP (green) and Red fluorescent protein fused with peroxisome targeting signal (red) were co-transfected into Vero cells. The protein intracellular localization was visualized using confocal fluorescent microscope. Nuclei were stained with DAPI (blue). No obvious colocalization between DEPP and peroxisomes was observed.

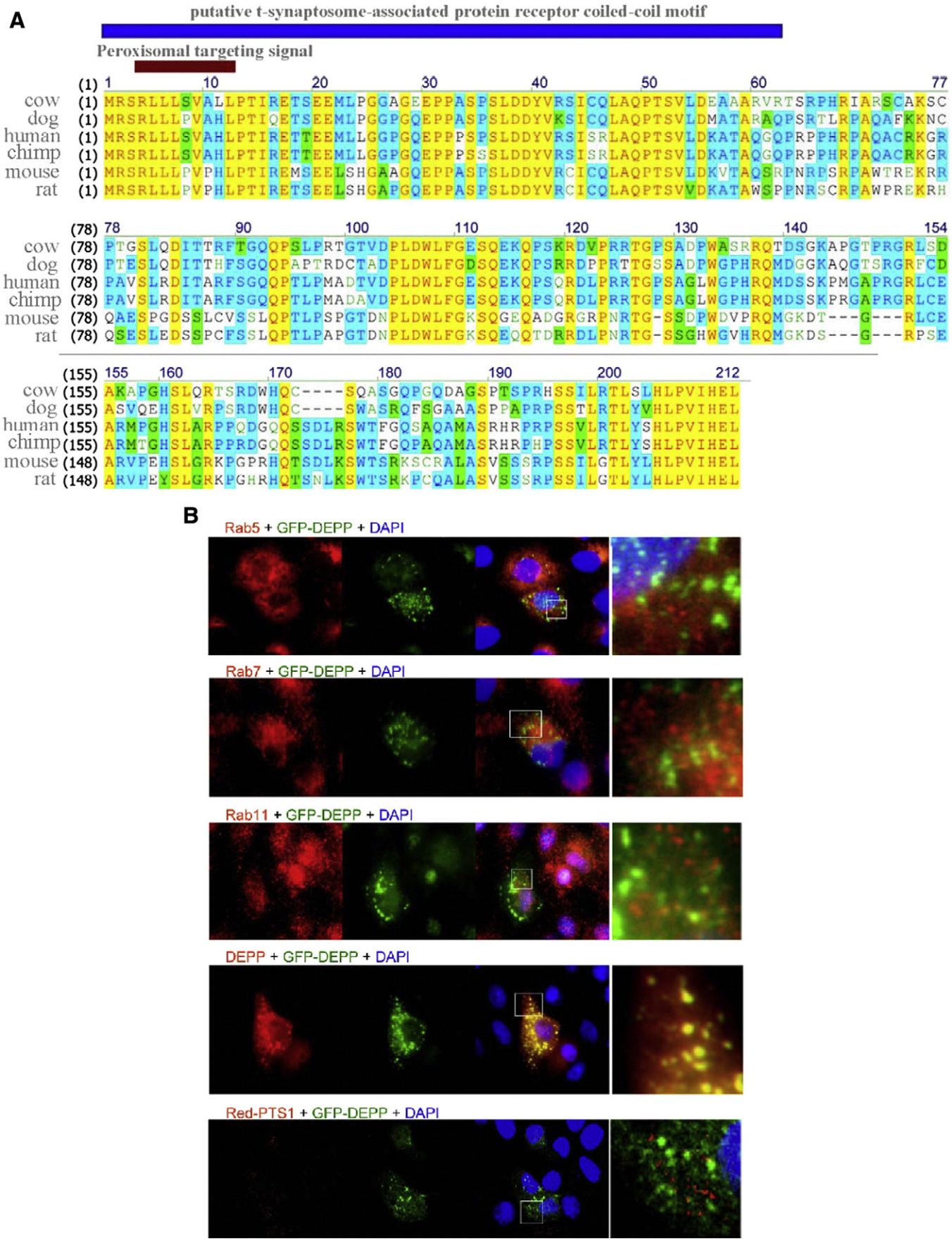
A
putative t-synaptosome-associated protein receptor coiled-coil motif
Peroxisomal targeting signal
cow
dog
human
chimp
mouse
rat
B
Rab5 + GFP-DEPP + DAPI
Rab7 + GFP-DEPP + DAPI
Rab11 + GFP-DEPP + DAPI
DEPP + GFP-DEPP + DAPI
Red-PTS1 + GFP-DEPP + DAPI

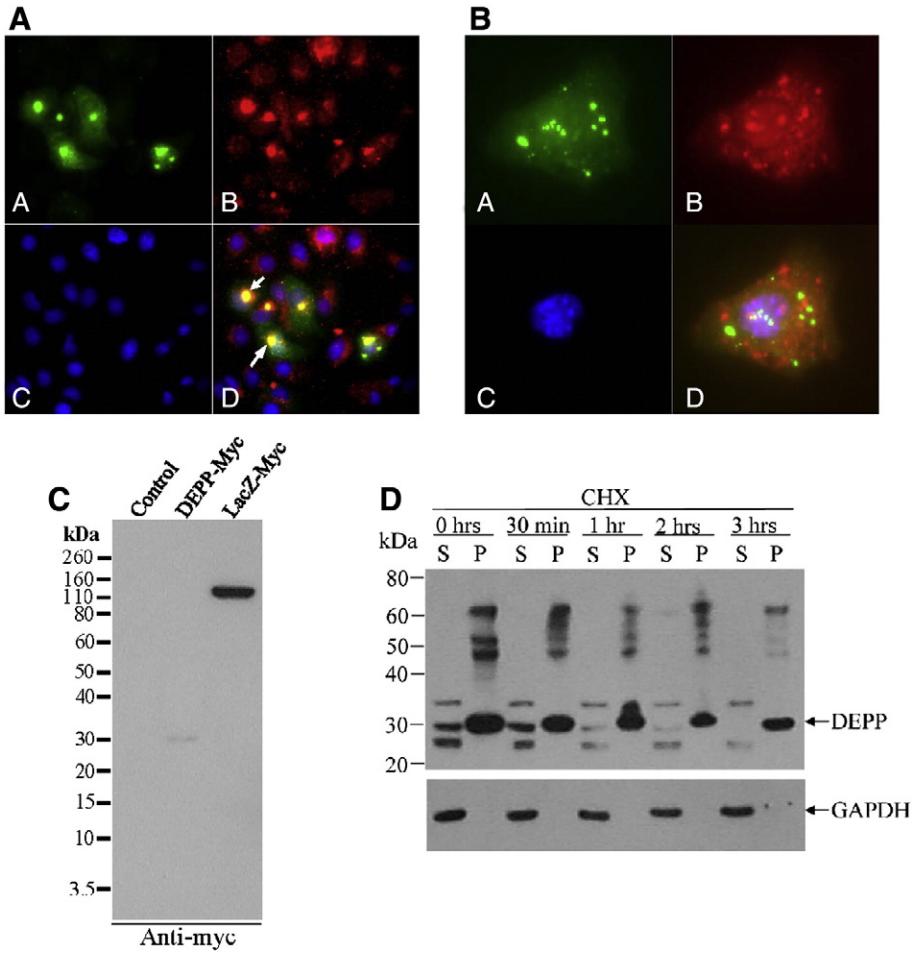

Fig. 6. Association of DEPP with aggresomes. A, Colocalization of DEPP with aggresomes. Vero cells were transfected with pEGFP-DEPP plasmid (panel A). Aggresomes were detected using ProteoStat Aggresome Detection Kit (see red staining in panel B). Nuclei were stained with DAPI (panel C). Images were merged in panel D. B, Staining Vero cells for DEPP and lysosomes. Vero cells were transfected with GFP-DEPP (A) and then incubated with LysoTracker Red (B). Nuclei were stained using Hoechst 33342 Nuclear Stain (C). Merged images shown in panel D. Images were acquired by fluorescent microscopy. C, Vero cells were mock transfected (Control) or transfected with fusion proteins DEPP-Myc and LacZ-Myc. Relative levels of analyzed proteins were detected using Western blot and antibodies specific for myc-epitope. D, Determination of half-life of DEPP overexpressed in Vero cells. Vero cells were transfected with pcDNA3.1-hDEPP-Myc-His plasmid and 18 h following transfection cells were exposed to 50 μg/mL of cycloheximide (CHX) for time indicated. The cytosolic soluble (S) precipitate (P) fractions were prepared as described in Materials and methods. Relative levels of analyzed proteins were detected using Western blot and antibodies specific for DEPP or GAPDH. GAPDH was used as control.

3.7. Stabilization of DEPP by inhibitors of protein degradation

Taking in consideration that DEPP undergoes rapid proteolysis, we analyzed the effect of proteosomal inhibition on DEPP stability. Exposure of Vero cells transfected with plasmid encoding DEPP to the proteasome inhibitors lactacystin and MG132 significantly increased the levels of mouse and human DEPP (Fig. 7A). Interestingly, exposure to the ubiquitin ligase E1 inhibitor (UBEI-41) produced additional slow migrating DEPP-specific bands (Fig. 7A and B). To analyze the effects of MG132 on the stability of DEPP in soluble and insoluble fractions, we exposed cells to MG132 for 1, 3 and 6 h and then isolated corresponding fractions from the treated cells. As expected, MG132 stabilized mostly the soluble DEPP and had little effect on insoluble DEPP levels (Fig. 7C).

3.8. DEPP and autophagy

Degradation of toxic protein aggregates is carried out by proteasomes and autophagy. Autophagy is the process whereby protein aggregates and damaged organelles are first engulfed by autophagosomal membranes, then fused to lysosomes followed by elimination. We tested our hypothesis that DEPP aggregates are cleared not only by proteasomes, but also by autophagy. We found that treatment of HEK293 cells overexpressing DEPP with the inhibitor of macroautophagy, 3-methyladenine, increased DEPP by 10-fold following 24 h incubation (Fig. 8A). In contrast, the same treatment did not change the levels of overexpressed beta-galactosidase protein (LacZ).

The regulation of DEPP expression by a variety of stimuli, including hypoxia and energy deprivation, suggests involvement of *m*ammalian *T*arget *O*f *R*apamycin (mTOR) signaling pathway. mTOR pathway integrates signals from energy deprivation and hypoxic exposures to regulate many processes, including autophagy, metabolism and protein synthesis. mTOR is represented by two complexes, mTORC1 and mTORC2. mTORC1 activity can be measured by analyzing the phosphorylation of ribosomal subunit S6 [50,51]. P70 S6 kinase is primarily responsible for S6 phosphorylation and requires the phosphorylation of threonine (Thr) 389 for its activation. We, therefore, exposed cells to hypoxia (1% O_2) for 4 h and analyzed mTORC1 activity by measuring phosphorylation of its downstream mediator, p70S6 kinase at Thr389. Hypoxia reduced the phosphorylation of p70S6K at Thr389 (Fig. 8C), as has been described before [52], while overexpression of DEPP did not affect the phosphorylation of p70S6K under normoxic or hypoxic conditions. The similar inability to activate mTORC1 pathway has been described for other aggregation prone proteins including mutant Htt, tau, α-synuclein and synphilin-1, despite their ability to recruit mTOR into aggresome formation [53]. At the same time, DEPP levels were significantly attenuated in hypoxia-treated cells possibly due to either an increased protein degradation or attenuated translation of RNA. It is well known that the mTOR pathway is the major regulator of autophagy [54]. Treatment of HEK293 cells with

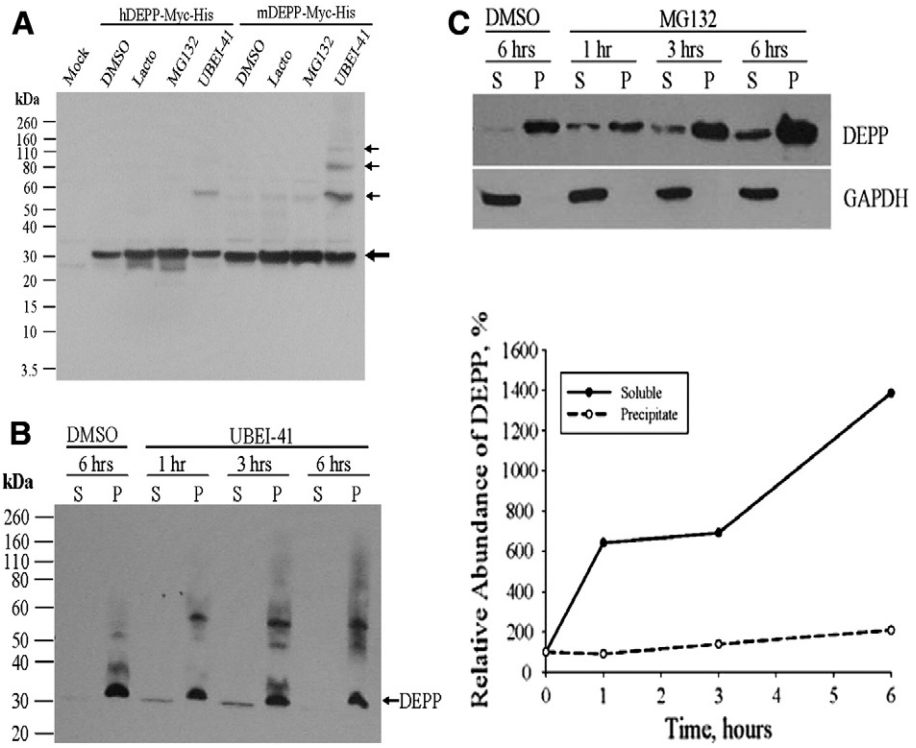

Fig. 7. Effect of ubiquitin ligase E1 (UBEI-41) and proteosomal (MG132) inhibitors on DEPP stability. A, Vero cells were transfected with plasmids encoding either mouse (mDEPP-Myc-His) or human (hDEPP-Myc-His) DEPP protein. Eighteen hours following transfections cells were exposed to 10 μM of lactacystin (lacto), 10 μM proteasomal inhibitor MG132 or 50 μM of ubiquitin ligase inhibitor UBEI-41. Cells were exposed for 6 h and whole cell lysates were analyzed using Western blot. B, Vero cells were transfected with pcDNA3.1-hDEPP-Myc-His plasmid and 18 h following transfection cells were exposed to 50 μM of UBEI-41 for time indicated. The cytosolic soluble (S) and precipitate (P) fractions were isolated and analyzed using Western blot. C, Vero cells were transfected with pcDNA3.1-hDEPP-Myc-His plasmid and 18 h following transfection cells were exposed to 10 μM MG132 for time indicated. The cytosolic soluble (S) precipitate (P) fractions were prepared as described in Materials and methods. Relative levels of analyzed proteins were detected using Western blot and antibodies specific for DEPP or GAPDH. GAPDH was used as control. Lower panel showed quantitative analysis of DEPP levels in soluble fractions or in precipitates.

an activator of autophagy and an inhibitor of mTOR pathway, rapamycin, attenuated levels of recombinant DEPP while inducing a specific marker of the autophagy LC3-II (Fig. 8B). Finally, overexpression of DEPP in HEK293 cells leads to activation of autophagy (Fig. 8D). Eighteen hours following transfection of DEPP encoding plasmid, levels of autophagy marker LC3 were significantly elevated compared to mock transfected cells. The treatment of cells with MG132 alone increased the intensities of LC3 bands as expected, while overexpression of DEPP and simultaneous treatment with MG132 increased the levels of the autophagy marker even further. These data indicate that DEPP steady-state levels in mammalian cells greatly depend on the activity of the autophagosomal degradation system. Moreover, we found that DEPP expression is able to induce autophagy in HEK293 cells. Next, we analyzed whether silencing of DEPP expression would affect autophagy. We found that Vero and HEK293 cells transfected with siRNA specific for DEPP had significantly lower steady-state levels of DEPP (Fig. 8E). This attenuation of DEPP expression in Vero cells reduced autophagy, as detected by the levels of LC3B autophagy marker (Fig. 8F). Surprisingly, no changes in autophagy were detected in HEK293 cells transfected with DEPP siRNA. We believe that this cell-specific effect of DEPP on autophagy is due to different expression levels of DEPP in HEK293 and Vero cells. We found that DEPP mRNA levels were 10-fold higher in Vero cells compared to HEK293 cells (Supplementary Fig. 2). Furthermore, the ratio LC3B/β-actin is two-fold higher in Vero cells compared to HEK293 cells (Fig. 8F, lower panel).

4. Discussion

In the present study, we investigated both the biological function of DEPP and its regulation by oxidative stress and hypoxia. We found that acute hypoxic stress significantly elevates DEPP mRNA levels in murine brain and kidney. We also found that a region 1000 bp upstream of the DEPP coding region is not involved in hypoxia-dependent induction but was sufficient for the activation of the DEPP promoter by EC-SOD. Computer analysis identified the hypoxia responsive element (HRE) 5′-CTAC GTGCTGC-3′ located in 3′-untranslated region of DEPP gene and its nucleotide sequence to be highly homologous to the HRE of erythropoietin gene. We believe that this HRE *cis*-element might be responsible for the short-term induction of DEPP by hypoxia, however additional experimental evidences are necessary.

DEPP expression in mammalian cells was induced by ectopic expression of Foxo1 and Foxo3a, but not by Foxo4 transcription factors. Our results are in a good agreement with previously published data reporting Foxo transcription factors as potent mediators of DEPP transcriptional activation in a renal adenocarcinoma cell line [55]. These transcriptional factors induce DEPP expression by binding to their putative binding sites within DEPP 5′-flanking region in human endothelial cells [56]. Foxo transcription factors regulate transcriptional responses to a variety of stresses including oxidative, nutrient and hormonal stresses [57]. Moreover, recently published data indicates that Foxo1 and Foxo3a are potent modulators of autophagy in transformed cells, cardiomyocytes and hematopoietic cells [58–60]. It is well known that reactive oxygen species regulate Foxo activity through both activating as well as repressing post-translational modifications, including phosphorylation, acetylation, ubiquitinylation, and methylation [61]. Thus, EC-SOD might regulate DEPP expression by modifying Foxo1 and Foxo3a transcription factors. It is also possible that EC-SOD exerts its effect on DEPP expression through elevation of hydrogen peroxide levels. Exogenous H_2O_2 is a potent stimulator of autophagy, but its effects on autophagy might be transduced through increased intracellular superoxide levels [62]. Thus, our data indicates that DEPP might be the important link for signal transduction pathways which convey extracellular oxidative stress signaling to the induction of autophagy.

We found that ectopically expressed DEPP co-localized with aggresomes. DEPP seems to form relatively large clusters of misfolded proteins and, at least in mammalian cells, is present in both soluble form and insoluble aggregates. Inhibition of 26S proteosomal machinery results in DEPPs' gradual accumulation in soluble and insoluble fractions, whereas inhibition of ubiquitin-activating enzyme E1 by UBEI-41, also known as PYR-41, facilitated the appearance of high molecular weight DEPP forms. We think that these high molecular weight

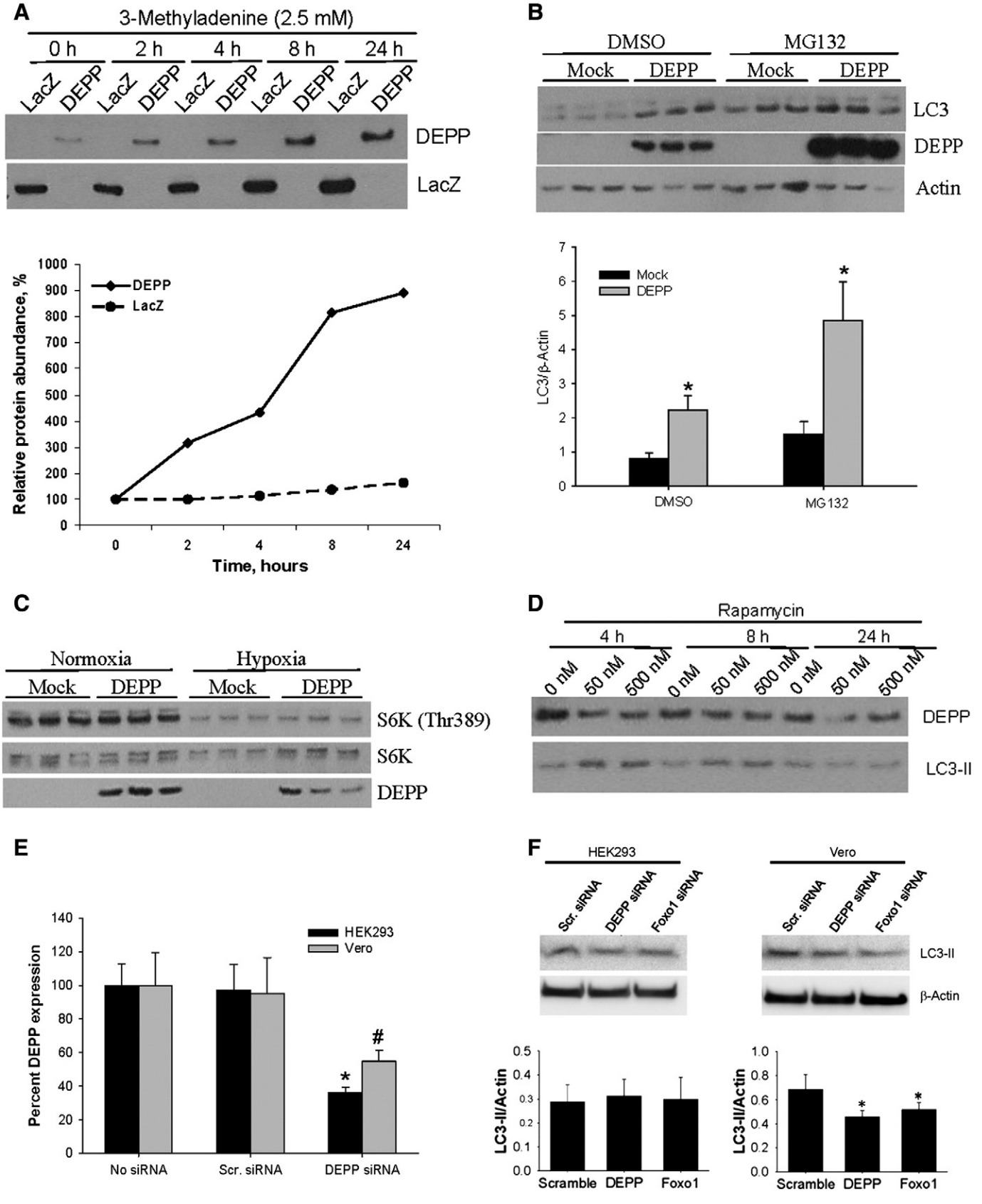

bands represent differently sumoylated and/or cross-linked oligomers of DEPP. UBEI-41, at concentration used in our experiments, should inhibit E1 dependent ubiquitylation by 95%, but it can also rapidly increase protein sumoylation [63] and protein cross-linking [64]. If degradation of DEPP is dependent on polyubiquitylation, then inhibition of this initial step of the ubiquitin cascade should increase DEPP protein levels. Indeed, the cumulative intensity of DEPP specific bands (including high molecular weight bands) significantly increased following exposure to UBEI-41 suggesting that ubiquitylation is the prerequisite step for DEPP degradation.

Abnormally folded polypeptides that escape proteasome-dependent degradation due to their large size can be transported via microtubules into aggresomes where they are stored and/or degraded by autophagy. If left unchecked, protein aggregates can cause cell toxicity leading to various pathologies, including major neurodegenerative diseases [65]. Thus, the active formation of aggresomes represents a protective cellular response to the accumulation of aggregated polypeptides when molecular chaperones and proteasomal machinery fail to handle misfolded protein waste. While we were unable to detect any toxic effect of DEPP on cell viability, we do not exclude the possibility of DEPP cytotoxicity under some specific conditions. For example, the toxicity of proteins with expanded polyglutamines is strongly enhanced by inhibition of the microtubule-dependent transport, which is required for aggresome formation [66].

One primary DEPP function suggested by our studies is the ability of DEPP to induce autophagy in mammalian cells. DEPP overexpression in HEK293 cells induces the association of microtubule-associated protein 1 (LC3-II isoform) with autophagic membranes, the first indication of autophagy upregulation. Moreover, silencing of DEPP expression in Vero cells attenuated autophagy. Taking into consideration that DEPP expression levels are more than 14 times higher in Vero cells compared to HEK293 cells, these cell-specific effects of DEPP on autophagy provide an additional confirmation of the important role DEPP plays in autophagy regulation. Furthermore, experiments using specific modulators of autophagy provide clear evidence for autophagic degradation of DEPP protein. Inhibition of autophagosome formation by 3-MA results in the elevated levels of DEPP even in the absence of proteosomal inhibitors, suggesting that autophagy is one of the main pathways involved in the degradation of DEPP inclusion bodies. On the other hand, activation of autophagy by rapamycin, decreases the levels of DEPP while concurrently upregulating LC3-II isoform (Fig. 8A and D).

What are the potential biological consequences of DEPP's ability to induce autophagy? The stress responsive expression of DEPP, and its ability to form aggregates in different cell lines, suggest that DEPP can participate in the development of a wide variety of human diseases associated with protein misfolding and/or impaired autophagic clearance. These diseases range from neurodegenerative disorders, such as Alzheimer and Parkinson's, to alcoholic and non-alcoholic hepatitis as well as several specific myopathies [67,68]. Autophagy-mediated clearance of neurotoxic aggregated proteins from aggresomes is a critical step in protecting neuronal cells from degeneration. This is the highly selective process as it has been shown that autophagy is involved in the clearance of mutant Huntington or tau proteins but not AIMP2 (p38) or mutant desmin [53]. The aggregation of unstable proteins can also be very cell-specific. For example, GPR37 protein overexpressed in the nigrostriatal system of rats, accumulated in an insoluble form in nigral neurons and nigrostriatal fibers, but not in GABAergic neurons. These GPR37 aggregates produce the permanent injury to the host neurons representing the clinical manifestation of juvenile Parkinsonism.

Is the ability of DEPP to activate autophagy a unique feature or is it a common phenomenon? It seems that several other proteins are able to activate autophagy. The similar activation of autophagy was observed following ectopic overexpression of aggregation-prone GPR37 protein [69]. Moreover, induction of protein aggregation in cardiomyocytes was a proximal signal for the activation of left ventricle autophagy in response to pressure overload [70]. Thus, upregulation of autophagy is, to some extent, a quite common response to aggresomal accumulation of misfolded proteins. However, the specificity of this process is not well understood. Nevertheless, the role of DEPP in the modulation of autophagosomal activity described here provides an additional insight into the complexity of these regulatory mechanisms.

Supplementary data to this article can be found online at http://dx.doi.org/10.1016/j.bbamcr.2014.02.003.

Acknowledgements

We would like to acknowledge the support of the Duke University DNA Microarray Facility. We thank Dr. Burgering (Utrecht University) for providing plasmids encoding the Foxo1, Foxo3a and Foxo4 transcription factors. This publication was made possible through the help of The Center for Environmental Genomics and Integrative Biology which is funded by NIH/NIEHS Grant Number P30ES014443 and through an internal grant from the University of Louisville, KY.

References

[1] T. Kietzmann, A. Gorlach, Reactive oxygen species in the control of hypoxia-inducible factor-mediated gene expression, Semin. Cell Dev. Biol. 16 (2005) 474–486.
[2] I. Fridovich, Superoxide anion radical ($O_2^{\cdot-}$), superoxide dismutases, and related matters, J. Biol. Chem. 272 (1997) 18515–18517.
[3] I.N. Zelko, T.J. Mariani, R.J. Folz, Superoxide dismutase multigene family: a comparison of the CuZn-SOD (SOD1), Mn-SOD (SOD2), and EC-SOD (SOD3) gene structures, evolution, and expression, Free Radic. Biol. Med. 33 (2002) 337–349.
[4] S.L. Marklund, Extracellular superoxide dismutase and other superoxide dismutase isoenzymes in tissues from nine mammalian species, Biochem. J. 222 (1984) 649–655.
[5] R.J. Folz, J.D. Crapo, Extracellular superoxide dismutase (SOD3): tissue-specific expression, genomic characterization, and computer-assisted sequence analysis of the human EC SOD gene, Genomics 22 (1994) 162–171.
[6] T. Ookawara, N. Imazeki, O. Matsubara, T. Kizaki, S. Oh-Ishi, C. Nakao, Y. Sato, H. Ohno, Tissue distribution of immunoreactive mouse extracellular superoxide dismutase, Am. J. Physiol. 275 (1998) C840–C847.
[7] J. Sandstrom, K. Karlsson, T. Edlund, S.L. Marklund, Heparin-affinity patterns and composition of extracellular superoxide dismutase in human plasma and tissues, Biochem. J. 294 (1993) 853–857.
[8] T.D. Oury, B.J. Day, J.D. Crapo, Extracellular superoxide dismutase in vessels and airways of humans and baboons, Free Radic. Biol. Med. 20 (1996) 957–965.
[9] L.M. Carlsson, J. Jonsson, T. Edlund, S.L. Marklund, Mice lacking extracellular superoxide dismutase are more sensitive to hyperoxia, Proc. Natl. Acad. Sci. U. S. A. 92 (1995) 6264–6268.
[10] R.J. Folz, A.M. Abushamaa, H.B. Suliman, Extracellular superoxide dismutase in the airways of transgenic mice reduces inflammation and attenuates lung toxicity following hyperoxia, J. Clin. Invest. 103 (1999) 1055–1066.

Fig. 8. DEPP is degraded by autophagy and is able to regulate autophagy. A, HEK293 cells were transfected either with plasmid encoding full-length not tagged DEPP or β-galactosidase (LacZ) and 18 h later were treated with inhibitor of autophagy 3-methyladenine for indicated time. Total cell lysates were isolated and analyzed by Western blot using antibodies specific for DEPP or for the myc tag attached to LacZ. Lower panel indicates quantitative analysis of relative abundance of proteins. B, DEPP overexpressed in HEK293 cells induced autophagy. HEK293 cells were mock transfected or transfected with plasmid encoding DEPP. On the next day cells were exposed to either DMSO or MG132 (10 μM) for 6 h and total cell lysates were analyzed using Western blot. Lower panel indicates quantitative analysis of relative abundance of proteins. Results shown are mean ± SD. $^{*}p < 0.05$; significant difference, *t*-test. C, Inhibition of mTOR pathway by hypoxia enhanced DEPP degradation. HEK293 cells were mock transfected or transfected with plasmid encoding DEPP. Cells were exposed to normobaric hypoxia (1% O_2, 5% CO_2) for 4 h. Total cell lysates were analyzed for the expression of DEPP and for dephosphorylation of p70 S6K at Thr389. D, Activation of autophagy by rapamycin reduces DEPP levels and increases LC3-II levels. HEK293 cells were transfected with plasmid encoding DEPP and then exposed to rapamycin for time indicated. Total cell lysates were analyzed for DEPP and LC3 levels using Western blot. E, Silencing of DEPP expression in HEK293 and Vero cells using siRNA. Cells were transfected with non-specific siRNA (Scr.) or DEPP specific siRNA. DEPP mRNA levels were analyzed 24 h after transfection using qRT-PCR. $^{*}p < 0.05$ compared to Scr. siRNA in HEK293 cells; $^{\#}p < 0.05$ compared to Scr. siRNA in Vero cells. F, Attenuation of autophagy in Vero cells transfected with DEPP and Foxo1 siRNA. LC3-II marker of autophagy was analyzed using Western blot and normalized to β-actin expression. Results shown are mean ± SD, N = 6, $^{*}p < 0.05$ compared to scrambled siRNA.

[11] M.N. Ahmed, H.B. Suliman, R.J. Folz, E. Nozik-Grayck, M.L. Golson, S.N. Mason, R.L. Auten, Extracellular superoxide dismutase protects lung development in hyperoxia-exposed newborn mice, Am. J. Respir. Crit. Care Med. 167 (2003) 400–405.
[12] M.F. Tsan, Superoxide dismutase and pulmonary oxygen toxicity: lessons from transgenic and knockout mice (review), Int. J. Mol. Med. 7 (2001) 13–19.
[13] H.B. Suliman, L.K. Ryan, L. Bishop, R.J. Folz, Prevention of influenza-induced lung injury in mice overexpressing extracellular superoxide dismutase, Am. J. Physiol. Lung Cell. Mol. Physiol. 280 (2001) L69–L78.
[14] A.J. Ghio, H.B. Suliman, J.D. Carter, A.M. Abushamaa, R.J. Folz, Overexpression of extracellular superoxide dismutase decreases lung injury after exposure to oil fly ash, Am. J. Physiol. Lung Cell. Mol. Physiol. 283 (2002) L211–L218.
[15] R.P. Bowler, J. Arcaroli, J.D. Crapo, A. Ross, J.W. Slot, E. Abraham, Extracellular superoxide dismutase attenuates lung injury after hemorrhage, Am. J. Respir. Crit. Care Med. 164 (2001) 290–294.
[16] R.P. Bowler, J. Arcaroli, E. Abraham, M. Patel, L.Y. Chang, J.D. Crapo, Evidence for extracellular superoxide dismutase as a mediator of hemorrhage-induced lung injury, Am. J. Physiol. Lung Cell. Mol. Physiol. 284 (2003) L680–L687.
[17] S.K. Kang, Z.N. Rabbani, R.J. Folz, M.L. Golson, H. Huang, D. Yu, T.S. Samulski, M.W. Dewhirst, M.S. Anscher, Z. Vujaskovic, Overexpression of extracellular superoxide dismutase protects mice from radiation-induced lung injury, Int. J. Radiat. Oncol. Biol. Phys. 57 (2003) 1056–1066.
[18] Z. Van Rheen, C. Fattman, S. Domarski, S. Majka, D. Klemm, K.R. Stenmark, E. Nozik-Grayck, Lung extracellular superoxide dismutase overexpression lessens bleomycin-induced pulmonary hypertension and vascular remodeling, Am. J. Respir. Cell Mol. Biol. 44 (2011) 500–508.
[19] R.P. Bowler, M. Nicks, K. Warnick, J.D. Crapo, Role of extracellular superoxide dismutase in bleomycin-induced pulmonary fibrosis, Am. J. Physiol. Lung Cell. Mol. Physiol. 282 (2002) L719–L726.
[20] C.L. Fattman, L.Y. Chang, T.A. Termin, L. Petersen, J.J. Enghild, T.D. Oury, Enhanced bleomycin-induced pulmonary damage in mice lacking extracellular superoxide dismutase, Free Radic. Biol. Med. 35 (2003) 763–771.
[21] Y. Kim, B.H. Kim, H. Lee, B. Jeon, Y.S. Lee, M.J. Kwon, T.Y. Kim, Regulation of skin inflammation and angiogenesis by EC-SOD via HIF-1alpha and NF-kappaB pathways, Free Radic. Biol. Med. 51 (2011) 1985–1995.
[22] I.N. Zelko, R.J. Folz, Extracellular superoxide dismutase functions as a major repressor of hypoxia-induced erythropoietin gene expression, Endocrinology 146 (2005) 332–340.
[23] H.B. Suliman, M. Ali, C.A. Piantadosi, Superoxide dismutase-3 promotes full expression of the EPO response to hypoxia, Blood 104 (2004) 43–50.
[24] H. Watanabe, K. Nonoguchi, T. Sakurai, T. Masuda, K. Itoh, J. Fujita, A novel protein Depp, which is induced by progesterone in human endometrial stromal cells activates Elk-1 transcription factor, Mol. Hum. Reprod. 11 (2005) 471–476.
[25] D. Shin, D.J. Anderson, Isolation of arterial-specific genes by subtractive hybridization reveals molecular heterogeneity among arterial endothelial cells, Dev. Dyn. 233 (2005) 1589–1604.
[26] B.T. Ragel, W.T. Couldwell, D.L. Gillespie, R.L. Jensen, Identification of hypoxia-induced genes in a malignant glioma cell line (U-251) by cDNA microarray analysis, Neurosurg. Rev. 30 (2007) 181–187 (discussion 187).
[27] K.E. Rieger, G. Chu, Portrait of transcriptional responses to ultraviolet and ionizing radiation in human cells, Nucleic Acids Res. 32 (2004) 4786–4803.
[28] I. Dahlman, K. Linder, E. Arvidsson Nordstrom, I. Andersson, J. Liden, C. Verdich, T.I. Sorensen, P. Arner, Changes in adipose tissue gene expression with energy-restricted diets in obese women, Am. J. Clin. Nutr. 81 (2005) 1275–1285.
[29] N. Yabuta, H. Onda, M. Watanabe, N. Yoshioka, I. Nagamori, T. Funatsu, S. Toji, K. Tamai, H. Nojima, Isolation and characterization of the TIGA genes, whose transcripts are induced by growth arrest, Nucleic Acids Res. 34 (2006) 4878–4892.
[30] H.T. Kim, G. Kong, D. Denardo, Y. Li, I. Uray, S. Pal, S. Mohsin, S.G. Hilsenbeck, R. Bissonnette, W.W. Lamph, K. Johnson, P.H. Brown, Identification of biomarkers modulated by the rexinoid LGD1069 (bexarotene) in human breast cells using oligonucleotide arrays, Cancer Res. 66 (2006) 12009–12018.
[31] Y. Kuroda, H. Kuriyama, S. Kihara, K. Kishida, N. Maeda, T. Hibuse, H. Nishizawa, M. Matsuda, T. Funahashi, I. Shimomura, Insulin-mediated regulation of decidual protein induced by progesterone (DEPP) in adipose tissue and liver, Horm. Metab. Res. 42 (2010) 173–177.
[32] B. Kornmann, N. Preitner, D. Rifat, F. Fleury-Olela, U. Schibler, Analysis of circadian liver gene expression by ADDER, a highly sensitive method for the display of differentially expressed mRNAs, Nucleic Acids Res. 29 (2001) E51–E61.
[33] F. Atienzar, H. Gerets, S. Dufrane, K. Tilmant, M. Cornet, S. Dhalluin, B. Ruty, G. Rose, M. Canning, Determination of phospholipidosis potential based on gene expression analysis in HepG2 cells, Toxicol. Sci. 96 (2007) 101–114.
[34] P. Nioi, B.K. Perry, E.J. Wang, Y.Z. Gu, R.D. Snyder, In vitro detection of drug-induced phospholipidosis using gene expression and fluorescent phospholipid based methodologies, Toxicol. Sci. 99 (2007) 162–173.
[35] H. Sawada, K. Takami, S. Asahi, A toxicogenomic approach to drug-induced phospholipidosis: analysis of its induction mechanism and establishment of a novel in vitro screening system, Toxicol. Sci. 83 (2005) 282–292.
[36] K.E. Bethin, Y. Nagai, R. Sladek, M. Asada, Y. Sadovsky, T.J. Hudson, L.J. Muglia, Microarray analysis of uterine gene expression in mouse and human pregnancy, Mol. Endocrinol. 17 (2003) 1454–1469.
[37] A.M. Cuervo, Autophagy: in sickness and in health, Trends Cell Biol. 14 (2004) 70–77.
[38] G. Petrovski, S. Das, B. Juhasz, A. Kertesz, A. Tosaki, D.K. Das, Cardioprotection by endoplasmic reticulum stress-induced autophagy, Antioxid. Redox Signal. 14 (2011) 2191–2200.
[39] I. Kim, S. Rodriguez-Enriquez, J.J. Lemasters, Selective degradation of mitochondria by mitophagy, Arch. Biochem. Biophys. 462 (2007) 245–253.
[40] W.A. Dunn Jr., J.M. Cregg, J.A. Kiel, I.J. van der Klei, M. Oku, Y. Sakai, A.A. Sibirny, O.V. Stasyk, M. Veenhuis, Pexophagy: the selective autophagy of peroxisomes, Autophagy 1 (2005) 75–83.
[41] P. Bruno, A. Calastretti, M. Priulla, L. Asnaghi, F. Scarlatti, A. Nicolin, G. Canti, Cell survival under nutrient stress is dependent on metabolic conditions regulated by Akt and not by autophagic vacuoles, Cell. Signal. 19 (2007) 2118–2126.
[42] F. Scarlatti, R. Granata, A.J. Meijer, P. Codogno, Does autophagy have a license to kill mammalian cells? Cell Death Differ. 16 (2009) 12–20.
[43] E.H. Baehrecke, Autophagy: dual roles in life and death? Nat. Rev. Mol. Cell Biol. 6 (2005) 505–510.
[44] A. Terman, B. Gustafsson, U.T. Brunk, Autophagy, organelles and ageing, J. Pathol. 211 (2007) 134–143.
[45] B. Levine, D.J. Klionsky, Development by self-digestion: molecular mechanisms and biological functions of autophagy, Dev. Cell 6 (2004) 463–477.
[46] R. Kiffin, U. Bandyopadhyay, A.M. Cuervo, Oxidative stress and autophagy, Antioxid. Redox Signal. 8 (2006) 152–162.
[47] V. Modur, R. Nagarajan, B.M. Evers, J. Milbrandt, FOXO proteins regulate tumor necrosis factor-related apoptosis inducing ligand expression. Implications for PTEN mutation in prostate cancer, J. Biol. Chem. 277 (2002) 47928–47937.
[48] H. Stenmark, V.M. Olkkonen, The Rab GTPase family, Genome Biol. 2 (2001) (REVIEWS3007).
[49] K. Zen, J. Biwersi, N. Periasamy, A.S. Verkman, Second messengers regulate endosomal acidification in Swiss 3T3 fibroblasts, J. Cell Biol. 119 (1992) 99–110.
[50] R.C. Hresko, M. Mueckler, mTOR.RICTOR is the Ser473 kinase for Akt/protein kinase B in 3T3-L1 adipocytes, J. Biol. Chem. 280 (2005) 40406–40416.
[51] D.D. Sarbassov, D.A. Guertin, S.M. Ali, D.M. Sabatini, Phosphorylation and regulation of Akt/PKB by the rictor–mTOR complex, Science 307 (2005) 1098–1101.
[52] W. Li, M. Petrimpol, K.D. Molle, M.N. Hall, E.J. Battegay, R. Humar, Hypoxia-induced endothelial proliferation requires both mTORC1 and mTORC2, Circ. Res. 100 (2007) 79–87.
[53] E.S. Wong, J.M. Tan, W.E. Soong, K. Hussein, N. Nukina, V.L. Dawson, T.M. Dawson, A.M. Cuervo, K.L. Lim, Autophagy-mediated clearance of aggresomes is not a universal phenomenon, Hum. Mol. Genet. 17 (2008) 2570–2582.
[54] C.H. Jung, S.H. Ro, J. Cao, N.M. Otto, D.H. Kim, mTOR regulation of autophagy, FEBS Lett. 584 (2010) 1287–1295.
[55] S. Ramaswamy, N. Nakamura, I. Sansal, L. Bergeron, W.R. Sellers, A novel mechanism of gene regulation and tumor suppression by the transcription factor FKHR, Cancer cell 2 (2002) 81–91.
[56] S. Chen, J. Gai, Y. Wang, H. Li, FoxO regulates expression of decidual protein induced by progesterone (DEPP) in human endothelial cells, FEBS Lett. 585 (2011) 1796–1800.
[57] K.N. Papanicolaou, Y. Izumiya, K. Walsh, Forkhead transcription factors and cardiovascular biology, Circ. Res. 102 (2008) 16–31.
[58] J. Zhou, W. Liao, J. Yang, K. Ma, X. Li, Y. Wang, D. Wang, L. Wang, Y. Zhang, Y. Yin, Y. Zhao, W.G. Zhu, FOXO3 induces FOXO1-dependent autophagy by activating the AKT1 signaling pathway, Autophagy 8 (2012) 1712–1723.
[59] A. Sengupta, J.D. Molkentin, K.E. Yutzey, FoxO transcription factors promote autophagy in cardiomyocytes, J. Biol. Chem. 284 (2009) 28319–28331.
[60] M.R. Warr, M. Binnewies, J. Flach, D. Reynaud, T. Garg, R. Malhotra, J. Debnath, E. Passegue, FOXO3A directs a protective autophagy program in haematopoietic stem cells, Nature 494 (2013) 323–327.
[61] P.L. de Keizer, B.M. Burgering, T.B. Dansen, Forkhead box o as a sensor, mediator, and regulator of redox signaling, Antioxid. Redox Signal. 14 (2011) 1093–1106.
[62] Y. Chen, M.B. Azad, S.B. Gibson, Superoxide is the major reactive oxygen species regulating autophagy, Cell Death Differ. 16 (2009) 1040–1052.
[63] Y. Yang, J. Kitagaki, R.M. Dai, Y.C. Tsai, K.L. Lorick, R.L. Ludwig, S.A. Pierre, J.P. Jensen, I.V. Davydov, P. Oberoi, C.C. Li, J.H. Kenten, J.A. Beutler, K.H. Vousden, A.M. Weissman, Inhibitors of ubiquitin-activating enzyme (E1), a new class of potential cancer therapeutics, Cancer Res. 67 (2007) 9472–9481.
[64] V. Kapuria, L.F. Peterson, H.D. Showalter, P.D. Kirchhoff, M. Talpaz, N.J. Donato, Protein cross-linking as a novel mechanism of action of a ubiquitin-activating enzyme inhibitor with anti-tumor activity, Biochem. Pharmacol. 82 (2011) 341–349.
[65] A.B. Meriin, M.Y. Sherman, Role of molecular chaperones in neurodegenerative disorders, Int. J. Hyperthermia 21 (2005) 403–419.
[66] J.L. Webb, B. Ravikumar, D.C. Rubinsztein, Microtubule disruption inhibits autophagosome–lysosome fusion: implications for studying the roles of aggresomes in polyglutamine diseases, Int. J. Biochem. Cell Biol. 36 (2004) 2541–2550.
[67] C.A. Ross, M.A. Poirier, Protein aggregation and neurodegenerative disease, Nat. Med. 10 (2004) S10–S17 (Suppl.).
[68] M.L. Costa, R. Escaleira, A. Cataldo, F. Oliveira, C.S. Mermelstein, Desmin: molecular interactions and putative functions of the muscle intermediate filament protein, Braz. J. Med. Biol. Res. 37 (2004) 1819–1830.
[69] D. Marazziti, C. Di Pietro, E. Golini, S. Mandillo, R. Matteoni, G.P. Tocchini-Valentini, Induction of macroautophagy by overexpression of the Parkinson's disease-associated GPR37 receptor, FASEB J. 23 (2009) 1978–1987.
[70] P. Tannous, H. Zhu, A. Nemchenko, J.M. Berry, J.L. Johnstone, J.M. Shelton, F.J. Miller Jr., B.A. Rothermel, J.A. Hill, Intracellular protein aggregation is a proximal trigger of cardiomyocyte autophagy, Circulation 117 (2008) 3070–3078.